Uncovering correlated phases in moiré materials: an ab initio approach to 2D continuum Hamiltonians

$WSe_2/MoSe_2$ moiré potential

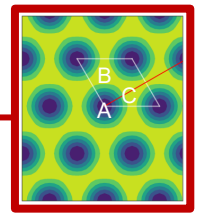

2306.14954

honeycomb moiré potential

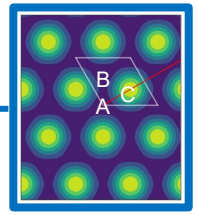

2406.01715

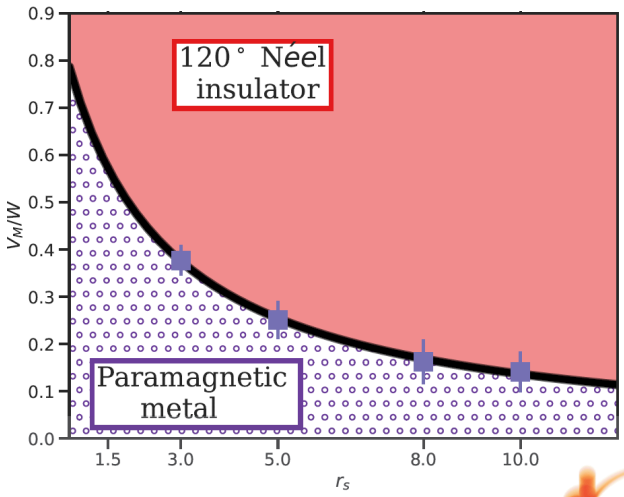

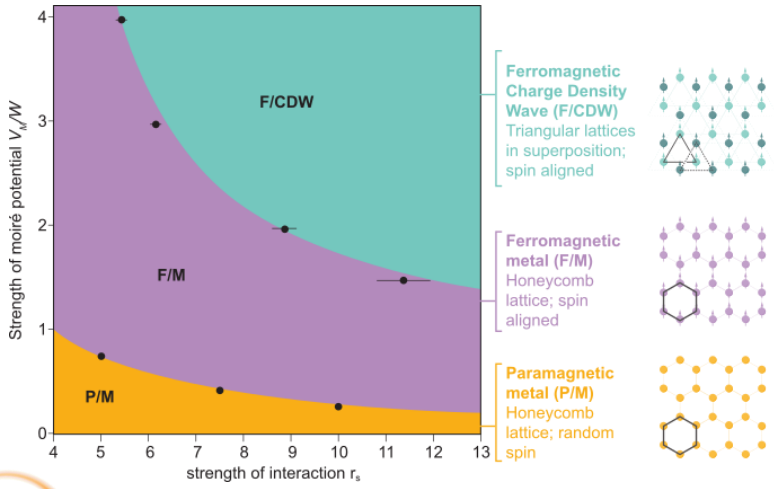

Miguel A. Morales

Shiwei Zhang

FLATIRON INSTITUTE

QUANTUMESPRESSO

QMCPACK

Yubo “Paul” Yang
Department of Physics and Astronomy, Hofstra University, Hempstead, NY 11549

HOFSTRA UNIVERSITY

Motivation: predict expt. and gain insight from computations

HOFSTRA UNIVERSITY

System

simulation cell

+ classical particles

+ quantum particles

Hamiltonian

H

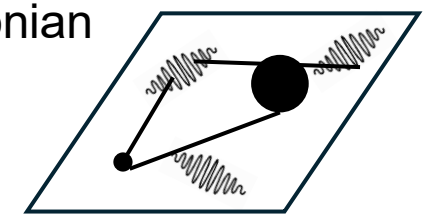

in silico Algorithm

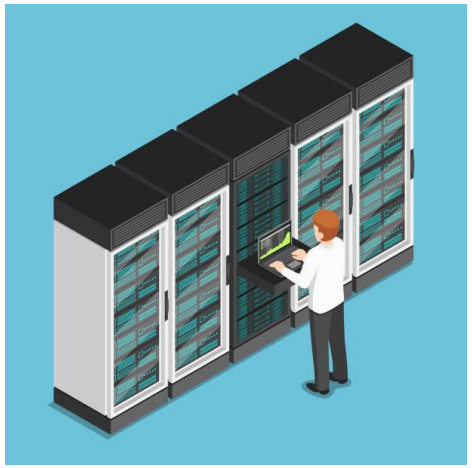

Calculate Observable

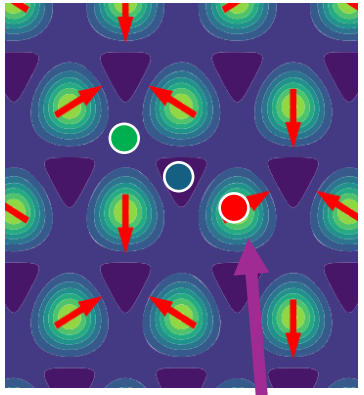

Charge density and spin orientations of electrons

Compute

Match charge

Predict spins

Y. Yang, M. Morales, S. Zhang, PRL **132**, 076503 (2024).

Material *in vivo*

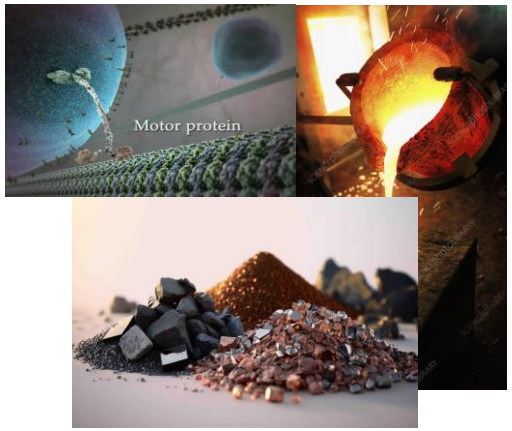

in vitro Experiment

Measure Property

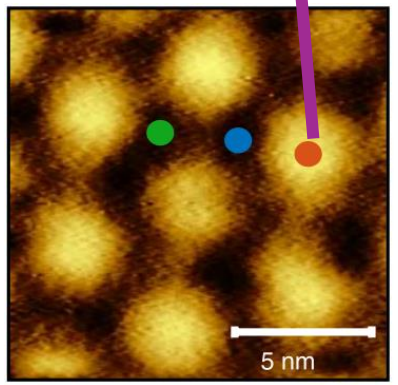

Scanning Tunneling Microscope (STM) image

Experiment

Sara Shabani (Columbia), Nat. Phys. **17**, 720 (2021).

Motivation: apply correlated methods to strongly correlated phases

- Many interesting phases in moiré materials are stabilized by strong electron interaction

PNAS **108**, 12233 (2011).
PRL **122**, 086402 (2019).

- Non-interacting continuum Hamiltonian, e.g., Bistritzer-MacDonald, predicted magic angle and topological phases
- Interacting continuum Hamiltonians are solved using **many-body methods designed for strong e-e interaction.**

Superconductivity in magic angle graphene

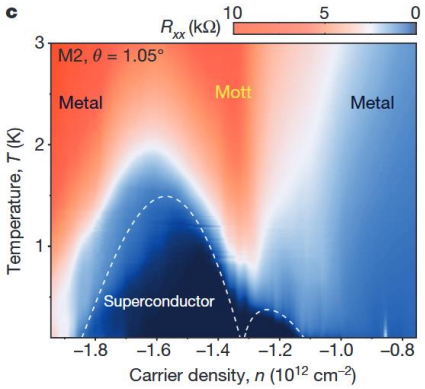

Nature **556**, 43 (2018).

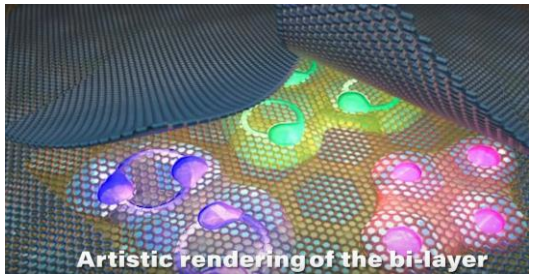

Seeker, YouTube

Superconductivity in twisted WSe_2

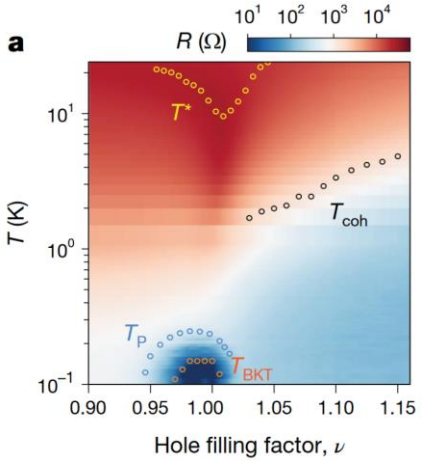

Nature **637**, 833 (2025).

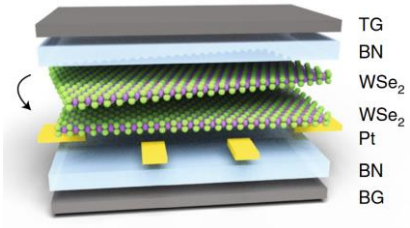

Nat. Matt. **19**, 861 (2020).

Fractional Chern insulator in pentalayer graphene and tMoTe2

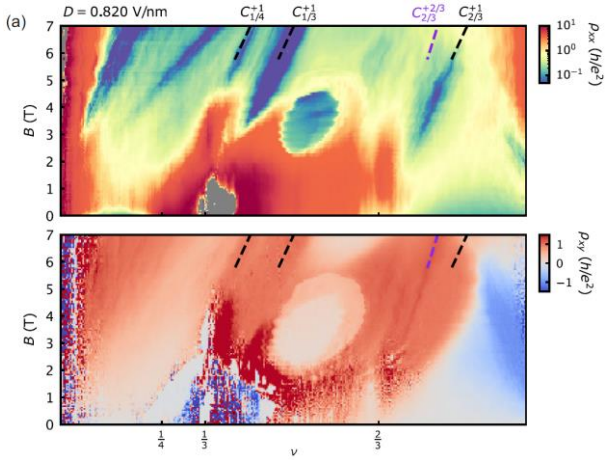

Phys. Rev. X, **15**, 011045 (2025)

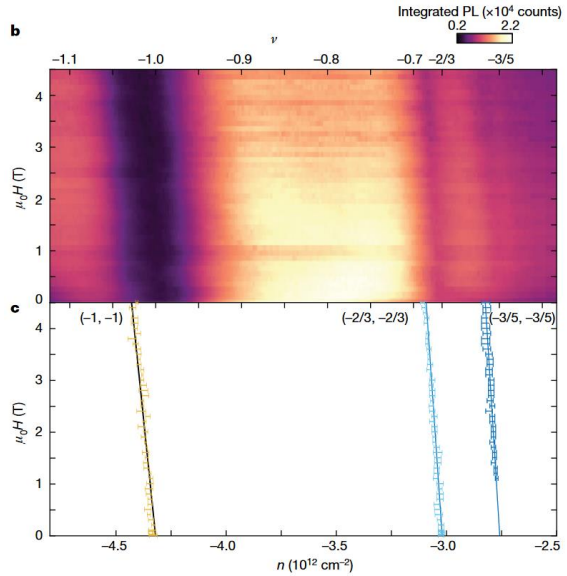

Nature, **622**, 64 (2023)

Semiconductor moiré continuum Hamiltonian is familiar

Similar to the usual ab initio Hamiltonian → existing precision many-body methods apply

For holes in a TMD heterobilayer such as $WSe_2/MoSe_2$:

$$H = \sum_{i=1}^{N} -\frac{\hbar^2}{2m^*}\nabla_i^2 - V_M \sum_{i,k} 2\cos(\boldsymbol{g}_k \cdot \boldsymbol{r}_i + \phi) + \frac{e^2}{4\pi\epsilon_0\epsilon_r}\sum_{i<j}\frac{1}{|r_i - r_j|} + b.g.$$

Kinetic energy at quadratic band edge

Moiré potential for each doped charge carrier

Coulomb interaction between all pairs of carriers

Without the moiré potential, this is an interacting 2D electron gas (2DEG)

moiré devices ← semiconductor heterobilayer ← 2DEG

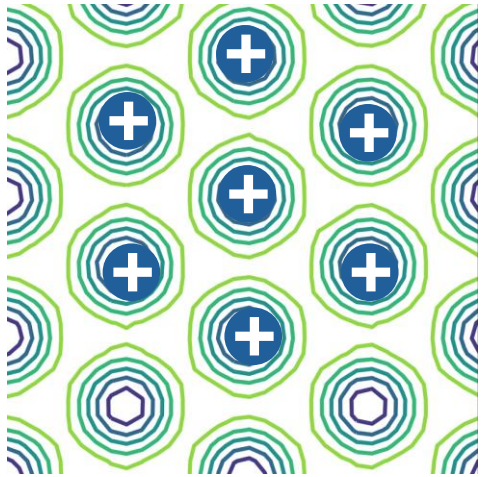

Surprisingly difficult to do accurate numerics on the electron gas

- Diffusion Monte Carlo (DMC) provided most accurate estimates of T=0 K transition densities

predicted Fermi liquid to Wigner crystal transition $r_s \sim 31 - 37$ in 2D and $r_s \approx 110$ in 3D

B. Tanatar and D.M. Ceperley, PRB **39**, 5005 (1989). 37 ± 5

N.D. Drummond and R.J. Needs, PRL **102**, 126402 (2009). 31 ± 1

S. Azadi, N.D. Drummond, S.M. Vinko, PRB **110**, 245145 (2024). 35 ± 1

C. Smith, Y. Chen *et al.*, PRL **133**, 266504 (2024). 37 ± 1

D.M. Ceperley and B.J. Alder, PRL **45**, 566 (1980).

M. Holzmann and S. Mononi, PRL **124**, 206404 (2020).

- Charge instability at the mean-field level challenges perturbative approaches

Hartree-Fock predicts crystal $r_s \approx 1.5$ in 2D and $r_s \approx 5$ in 3D

B. Bernu, F. Delyon, M. Holzmann, and L. Baguet, PRB **84**, 115115 (2011).

J.R. Trail, M.D. Towler, and R.J. Needs, PRB **68**, 045107 (2003).

Diagrammatic perturbation diverges around similar densities

K. Chen and K. Haule, Nat. Comm. **10**, 3725 (2019).

CCSDTQ5 needed for accurate result at $r_s = 5$ in 3D

V.A. Neufeld and A.J.W. Thom, J. Chem. Phys. **147**, 194105 (2017).

Semiconductor moiré continuum Hamiltonian is familiar

Similar to the usual ab initio e^- Hamiltonian → existing precision many-body methods apply

For holes in a TMD heterobilayer such as $WSe_2/MoSe_2$:

$$H = \sum_{i=1}^{N} -\frac{\hbar^2}{2m^*}\nabla_i^2 \; - V_M \sum_{i,k} 2\cos(\boldsymbol{g}_k \cdot \boldsymbol{r}_i + \phi) \; + \frac{e^2}{4\pi\epsilon_0\epsilon_r}\sum_{i<j}\frac{1}{|r_i - r_j|}$$

Kinetic energy at quadratic band edge

Moiré potential for each doped charge carrier

Coulomb interaction between all pairs of carriers

kinetic $W \equiv \dfrac{\hbar^2}{2m^* a^2}$ interaction $U \equiv \dfrac{e^2}{4\pi\epsilon_0\epsilon_r\, a}$

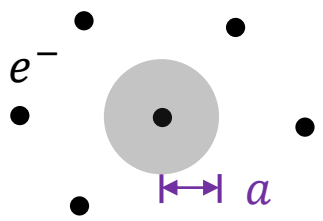

- Wigner-Seitz $r_s = U/W = a/a_B^*$ controls interaction strength
- V_M/W measures moiré strength
- ϕ changes the shape of the morié potential

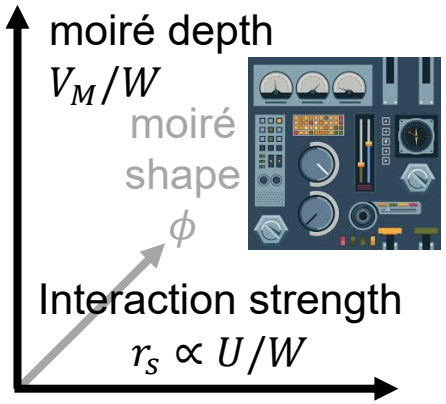

TMD bilayer is a semiconductor interface → 2DEG + moiré potential

Band edge energy is a function of stacking registry

Stacking changes due to moiré pattern → band edge energy shifts in moiré unit cell

→ modify the one-body part of the Hamiltonian (effective moiré potential)

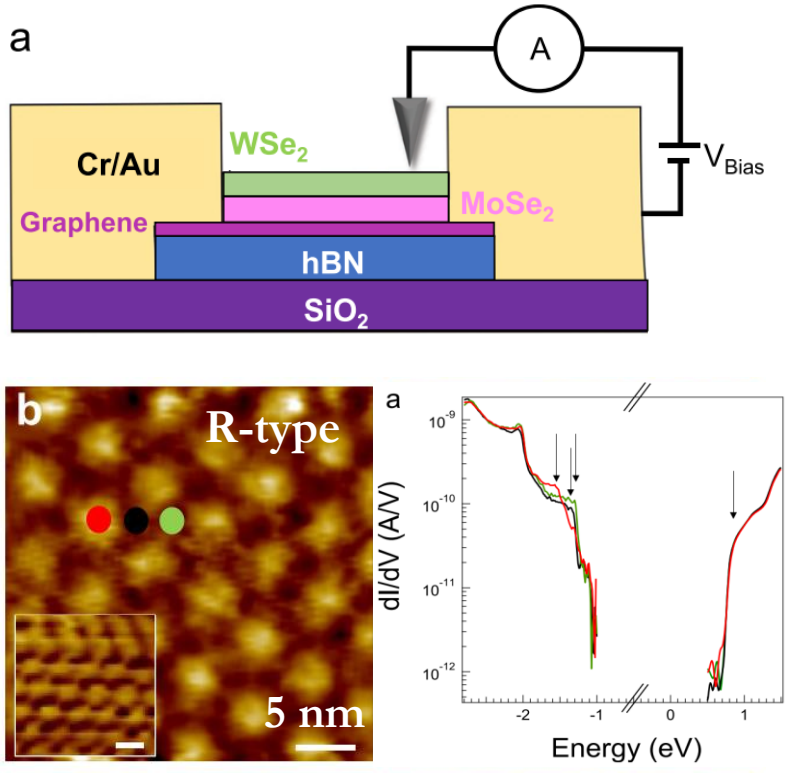

1. Map using STM/STS

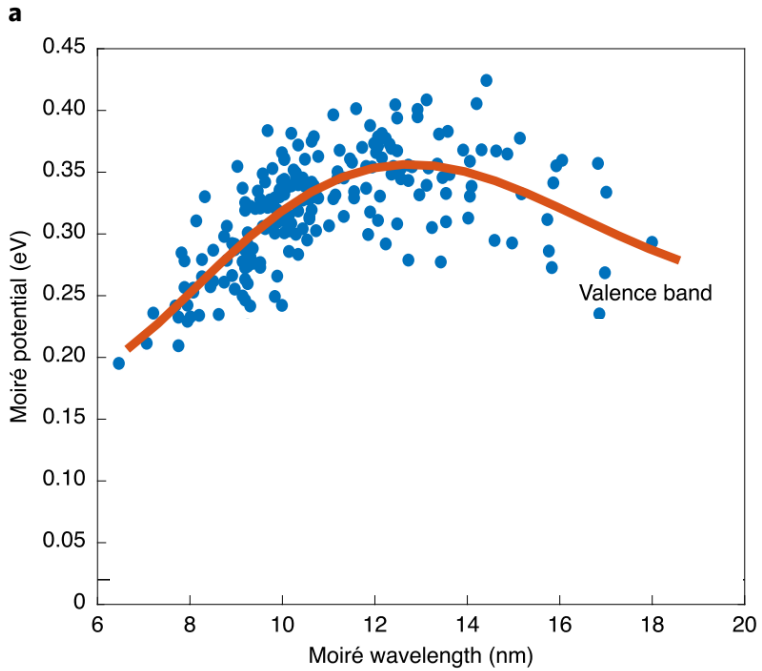

2. Model using large-scale DFT

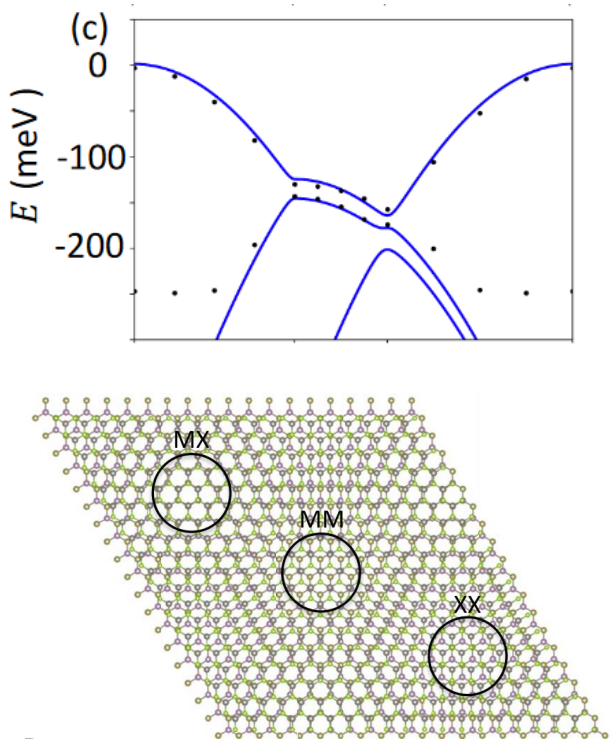

Rachel Nieken et al., APL Mater. **10** (2022)

Sara Shabani et al., Nat. Phys. **17** (2021)

Yang Zhang et al., PRB 102, 201115(R) (2020).

The simplest moiré potential (depth V_M, shape ϕ)

First shell of reciprocal lattice vectors $\boldsymbol{g}_k$

Require real-valued potential and C_3 rotation symmetry

$$V(\boldsymbol{r}) = \sum_{k=1}^{6} V(\boldsymbol{g}_k)\exp(i\,\boldsymbol{g}_k\cdot\boldsymbol{r}) = \sum_{k=1}^{6} V_M e^{i\phi}\exp(i\,\boldsymbol{g}_k\cdot\boldsymbol{r}) = V_M\sum_{k=1}^{3} 2\cos(i\,\boldsymbol{g}_{2k-1}\cdot\boldsymbol{r}+\phi)$$

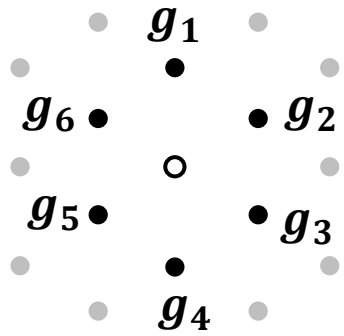

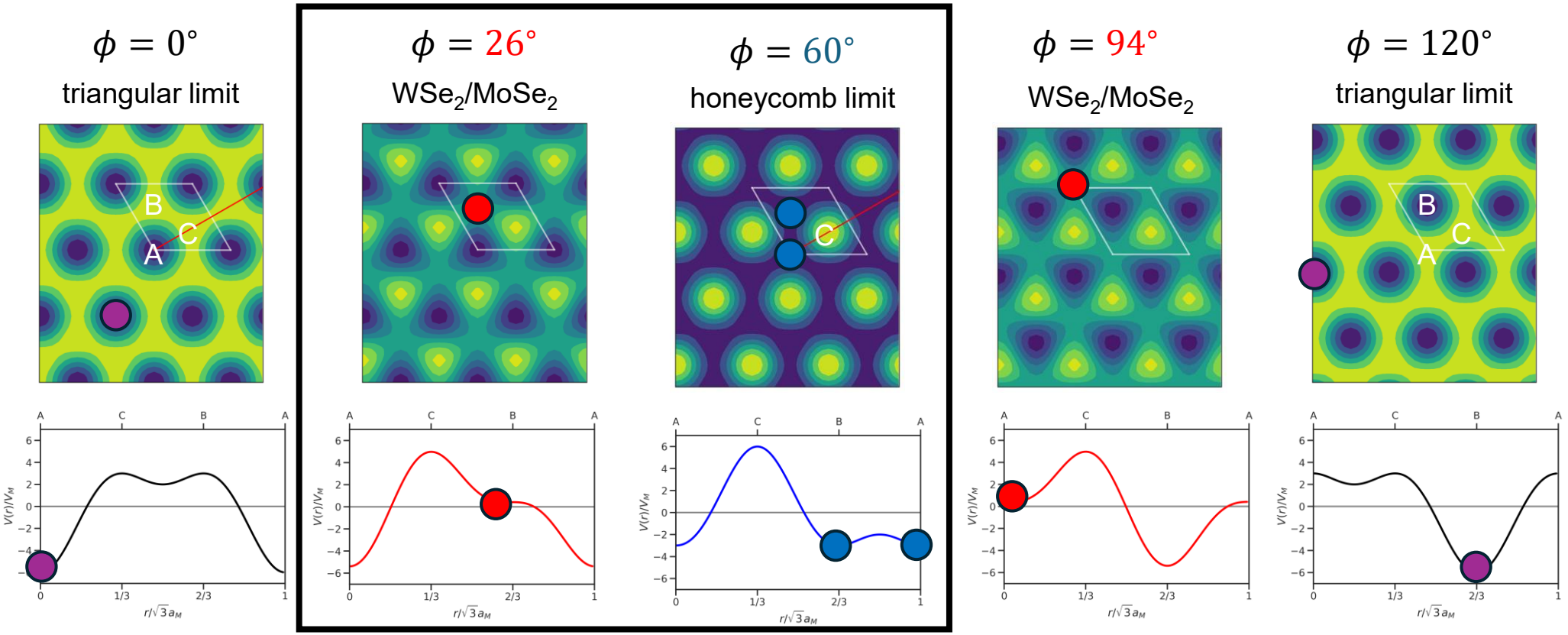

F. Wu, T. Lovorn, E. Tutuc, A. H. MacDonald, "Hubbard Model Physics in Transition Metal Dichalcogenide Moiré Bands," Phys. Rev. Lett. **121**, 026402 (2018).

Effect of the moiré potential: triangular charge and spin density waves

HOFSTRA UNIVERSITY

Triangular moiré potential commensurate with the triangular Wigner crystal (WC):

- Pin WC at higher density
- Strong AFM interaction

triangar-ish

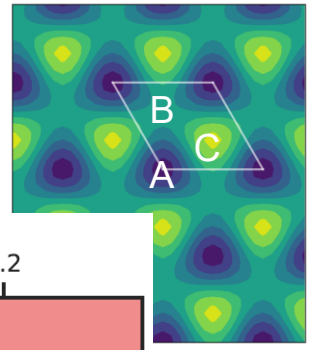

QMC phase diagram

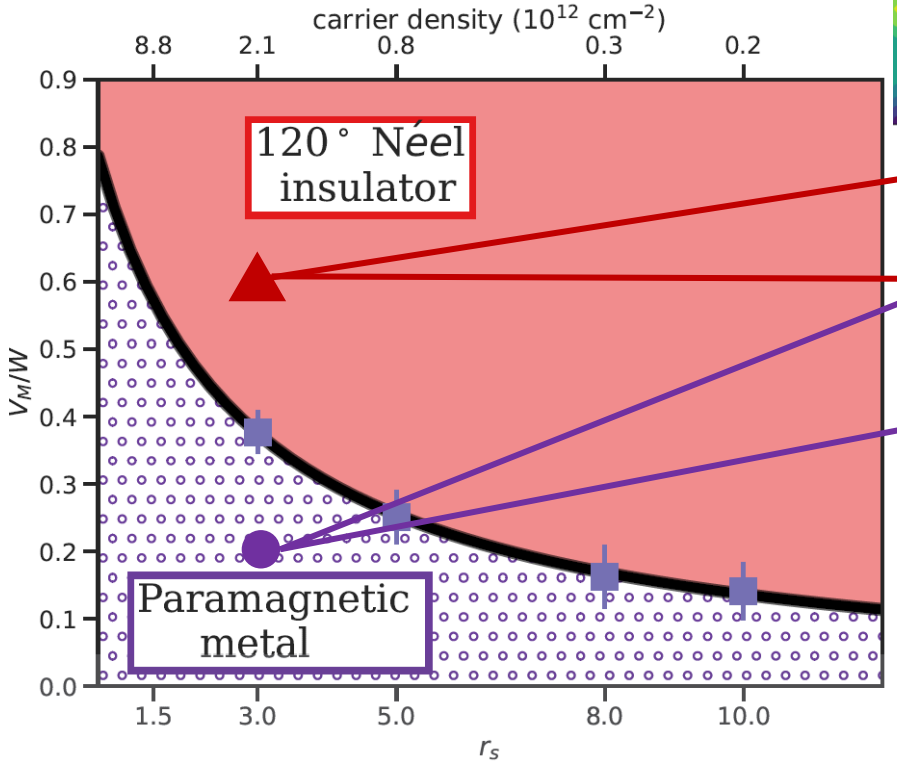

charge density

linecut

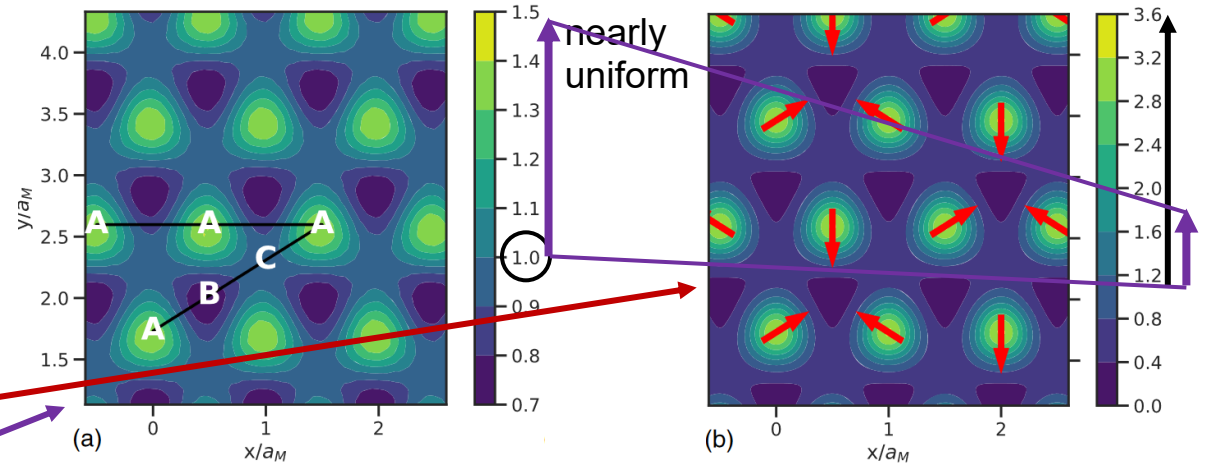

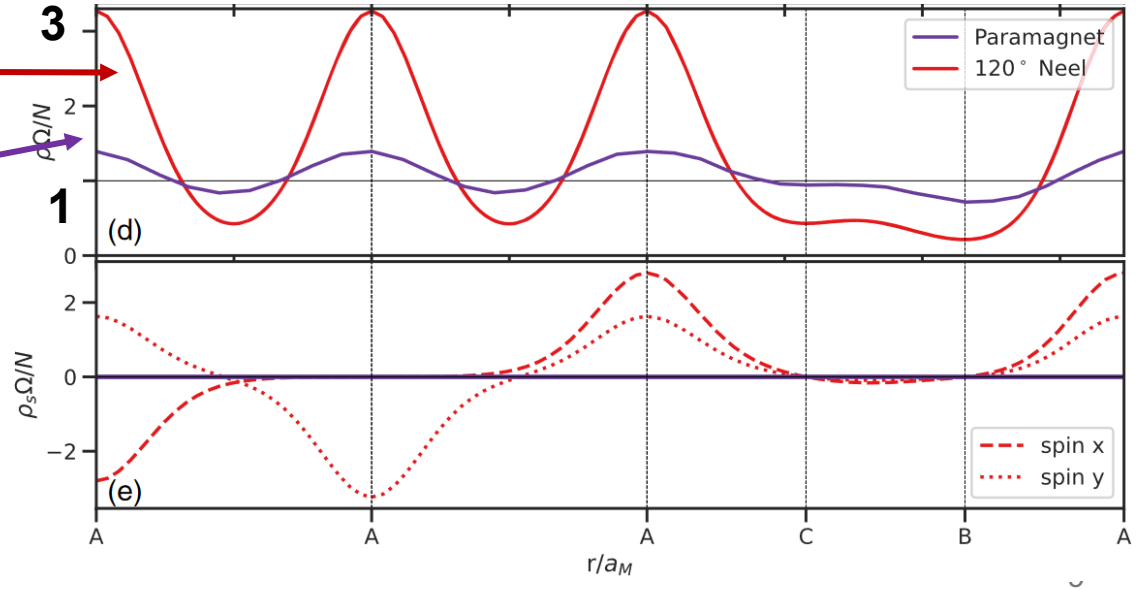

Y. Yang, M.A. Morales, S. Zhang, Phys. Rev. Lett. **132**, 076503 (2024).

Synergy between DFT and QMC → tune density functional

Charge density linecuts at r_s=3 across metal-insulator transition

- HF over-stabilizes charge order
- LDA under-stabilizes charge order
- Hybrid LDA and QMC show abrupt change in charge density across MIT

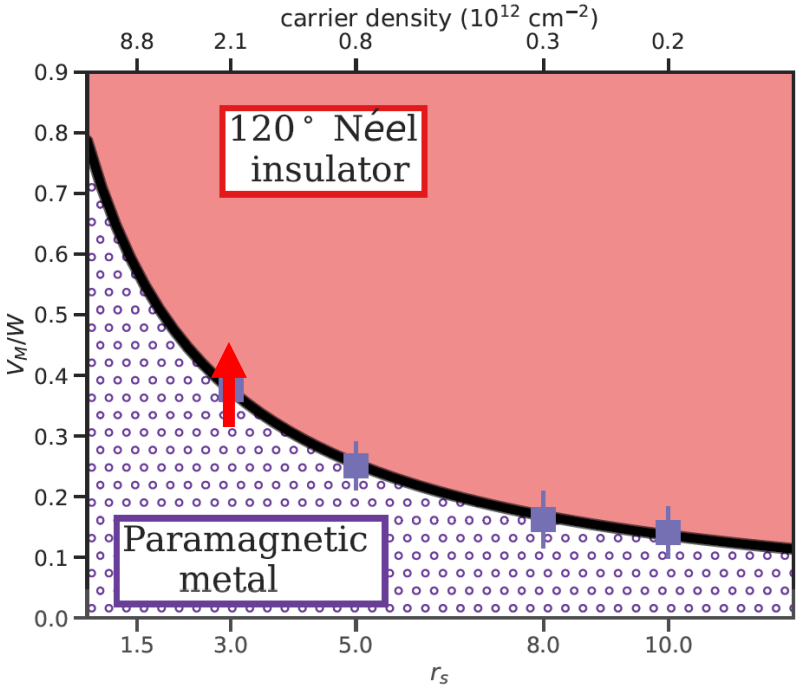

HF

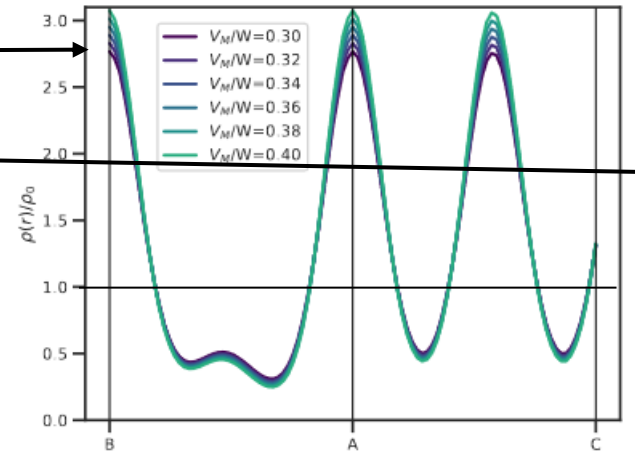

LDA

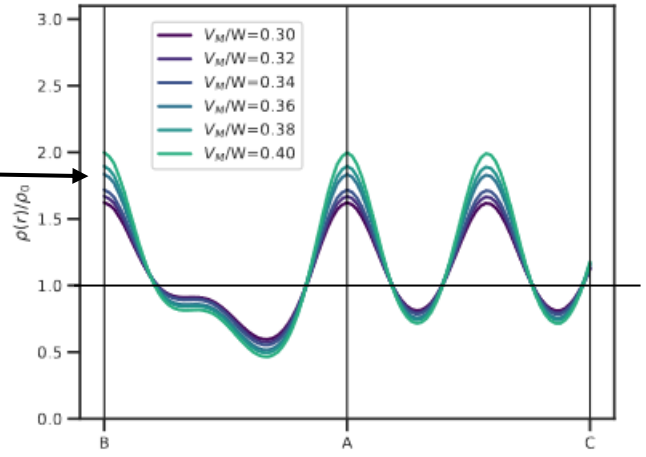

QMC

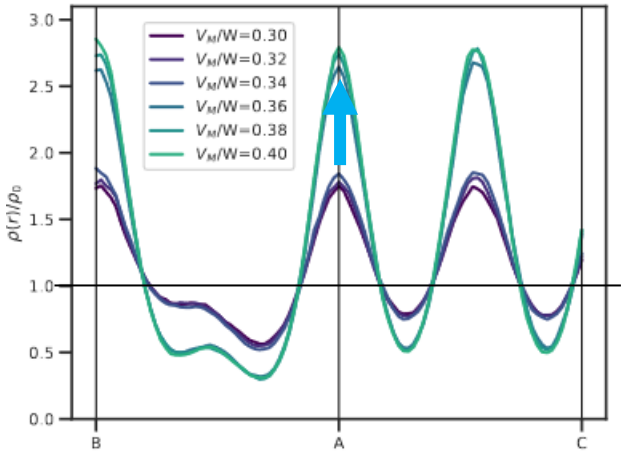

Becke's half-and-half

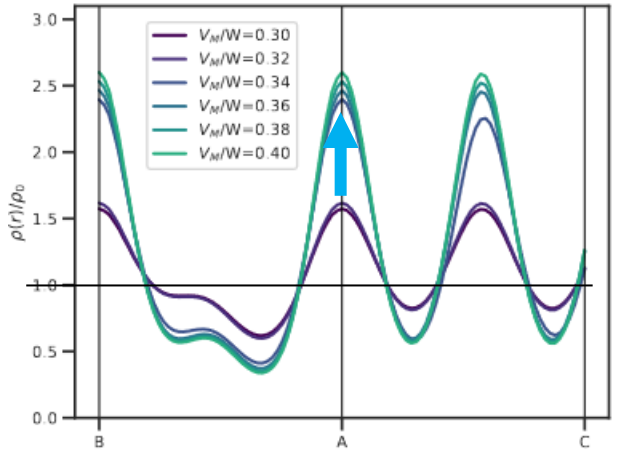

Y. Yang, M.A. Morales, S. Zhang, Phys. Rev. Lett. **132**, 076503 (2024).

A.D. Becke, J Chem Phys **98**, 1372 (1993)

Comparison to other approximations: understand region of applicability

Hartree Fock

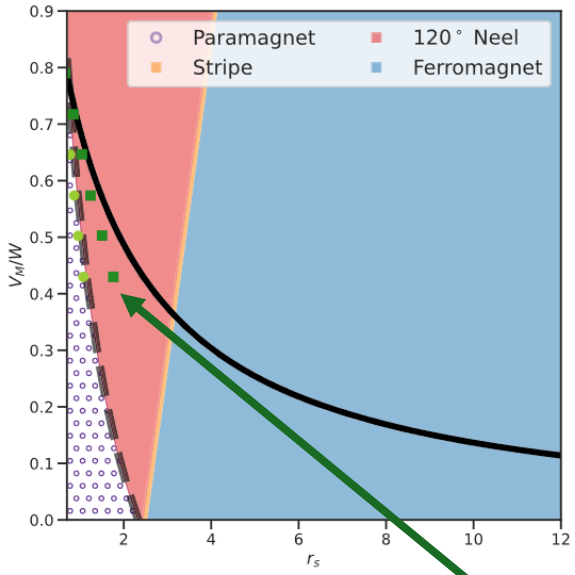

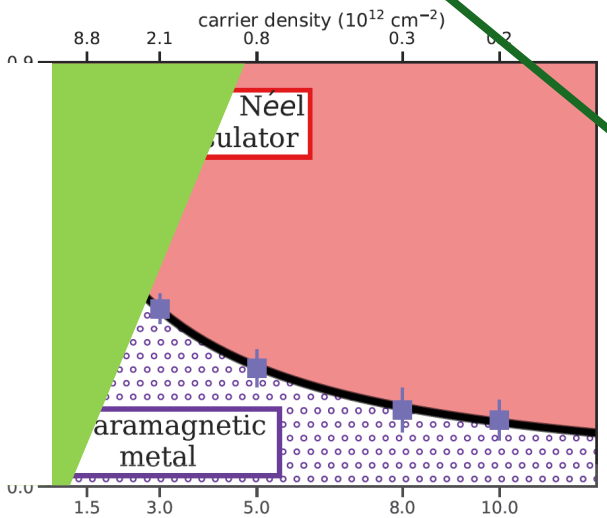

LDA

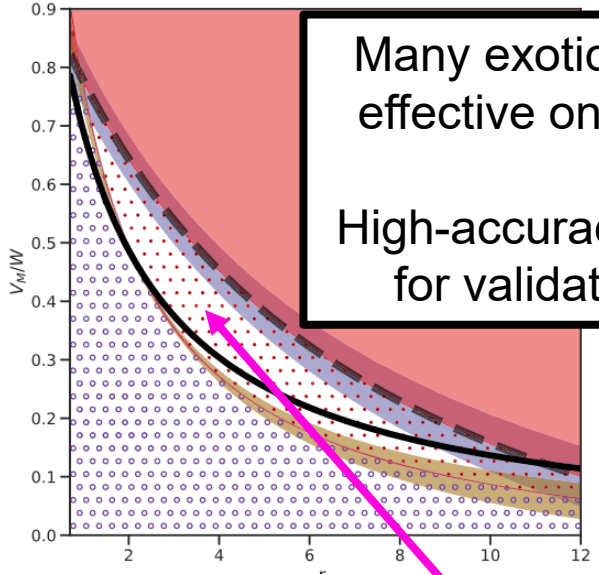

LDA + 50% exact exch.

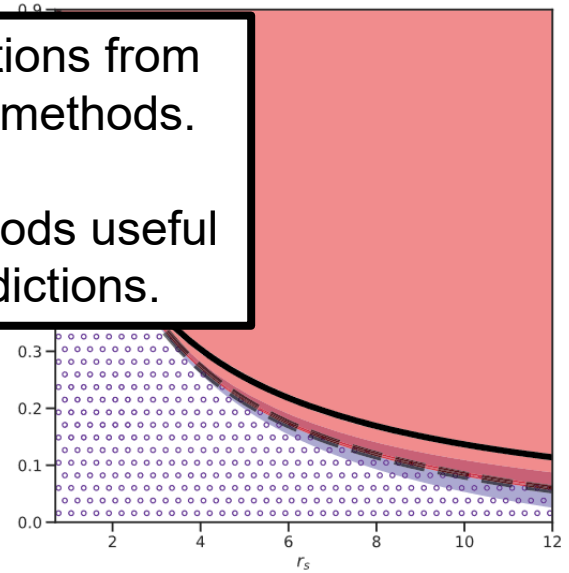

Many exotic predictions from effective one-body methods.

High-accuracy methods useful for validating predictions.

- HF over-stabilizes charge order and ferro.
- ED is accurate in deep moiré, but bias grows in shallower potential
- LDA over-stabilizes metallic phase: intermediate spin density wave (SDW) phase is not physical
- Hybrid LDA can be tuned to reproduce the QMC phase diagram.

Y. Yang, M.A. Morales, S. Zhang, Phys. Rev. Lett. **132**, 076503 (2024).

QMC as gatekeeper for unphysical “exotic predictions”

LDA self-interaction error: one electron pushes itself apart favors metallic phase

Alleviate using non-local hybrid functional $E_{xc}^{hybrid} = \alpha E_x^{HF} + (1-\alpha)E_x^{LDA} + E_c^{LDA}$

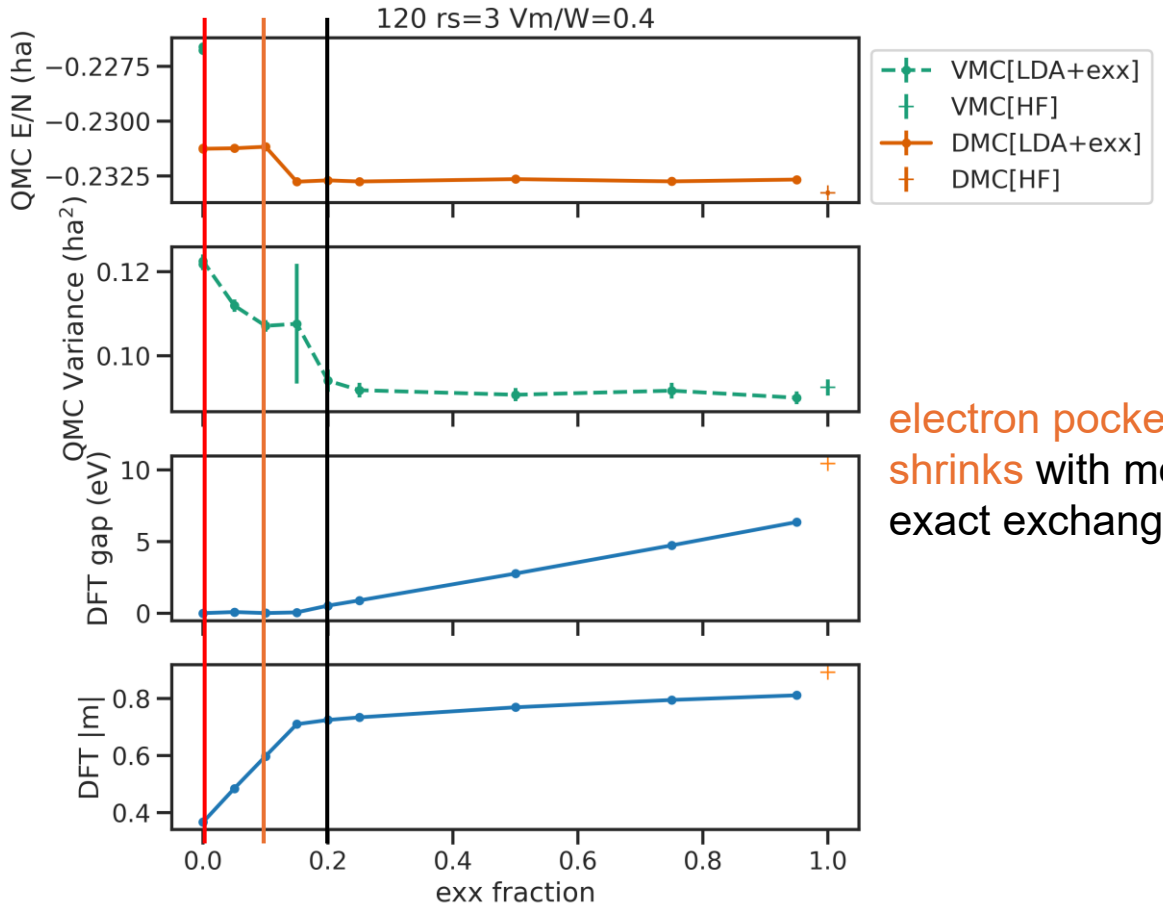

electron pockets shrinks with more exact exchange

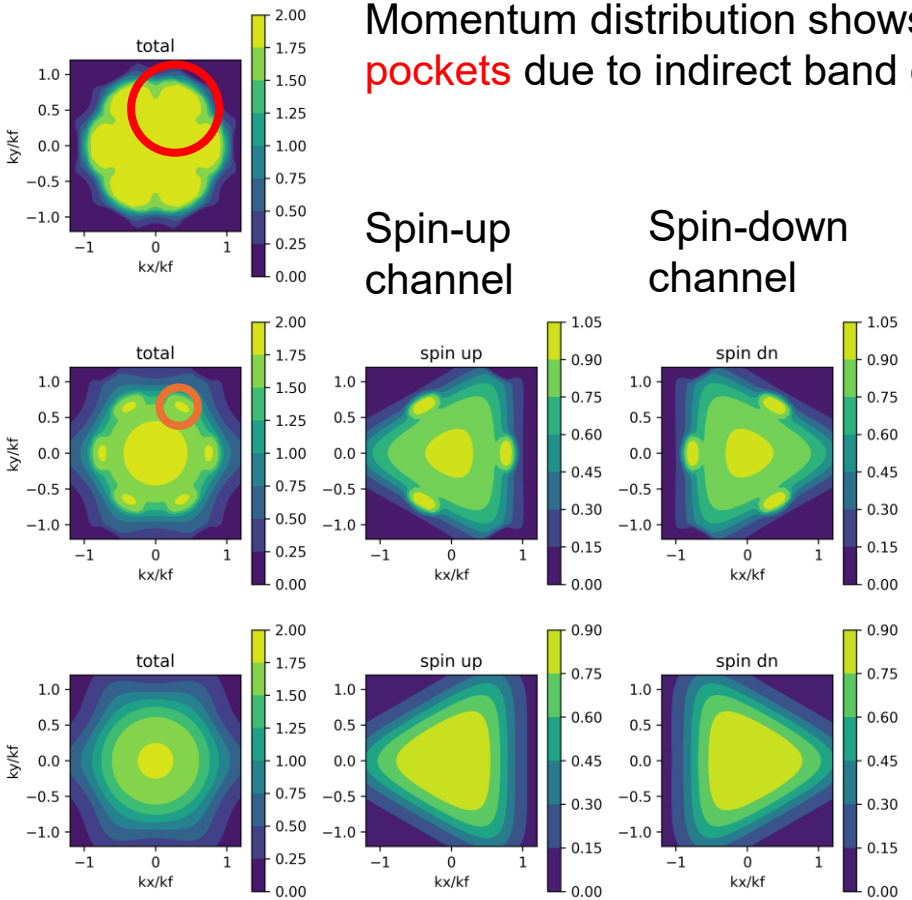

Momentum distribution shows electron pockets due to indirect band gap closure

Spin-up channel

Spin-down channel

Finite-size correction to remove effects of momentum discretization

- Known long-wavelength behavior of the static structure factor enables a finite-size correction
- QMC energy calculated with N=144 electrons can be corrected to match the thermodynamic limit

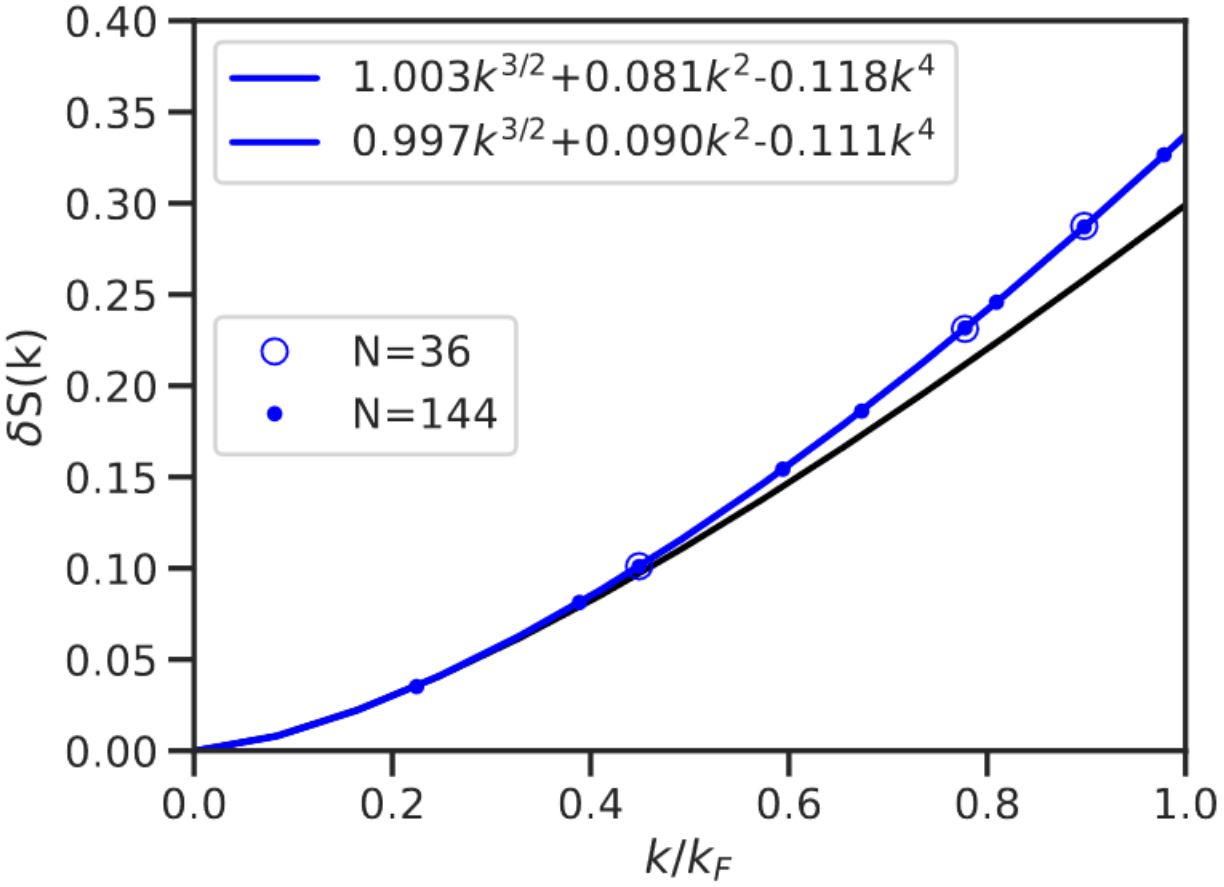

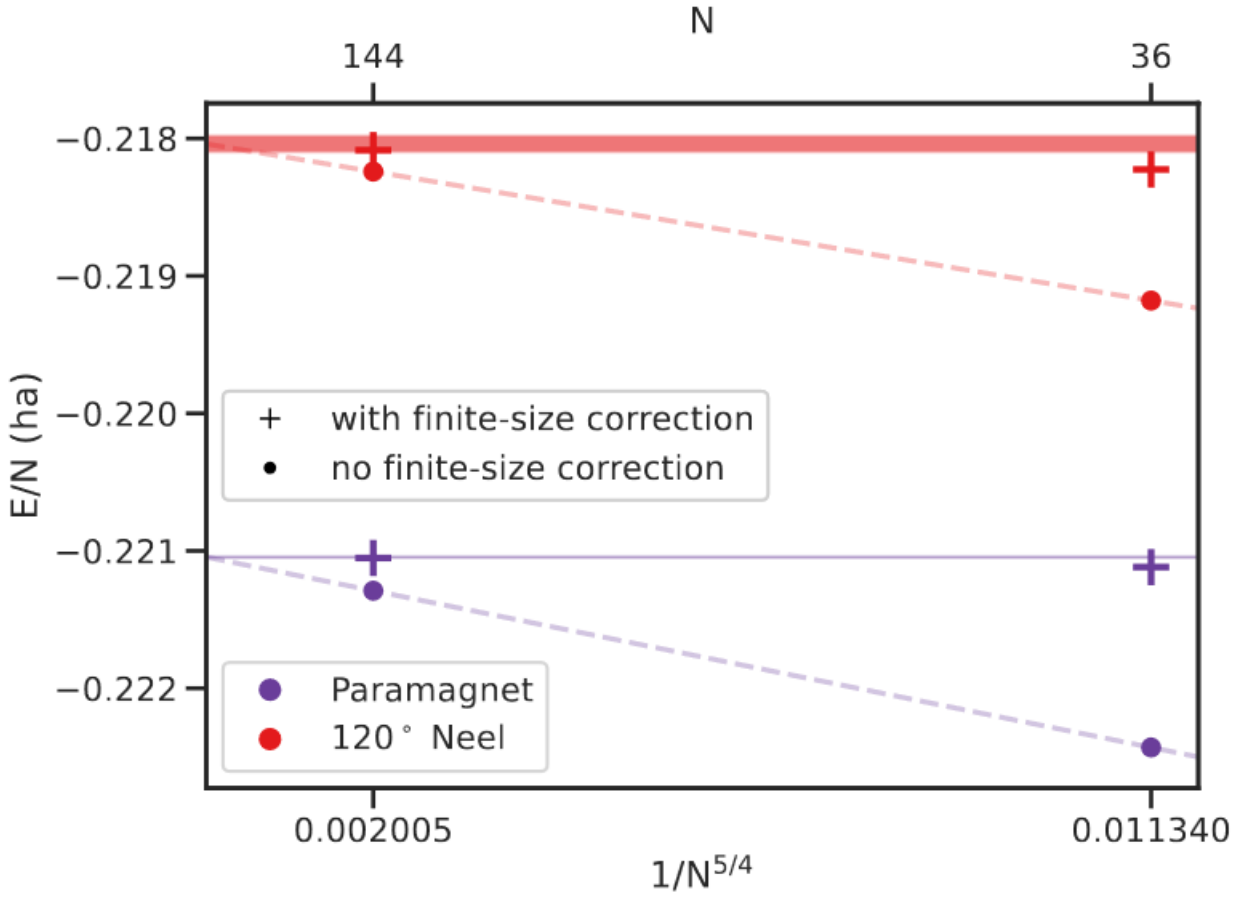

M. Holzmann, R. C. Clay III, M. A. Morales, N. M. Tubman, D. M. Ceperley, and C. Pierleoni, Phys. Rev. B **94**, 035126 (2016)

Effect of the moiré potential: honeycomb ferromagnetic semimetal

HOFSTRA UNIVERSITY

Honeycomb moiré potential favors ferromagnetism

honeycomb limit

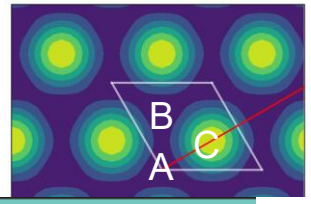

QMC phase diagram

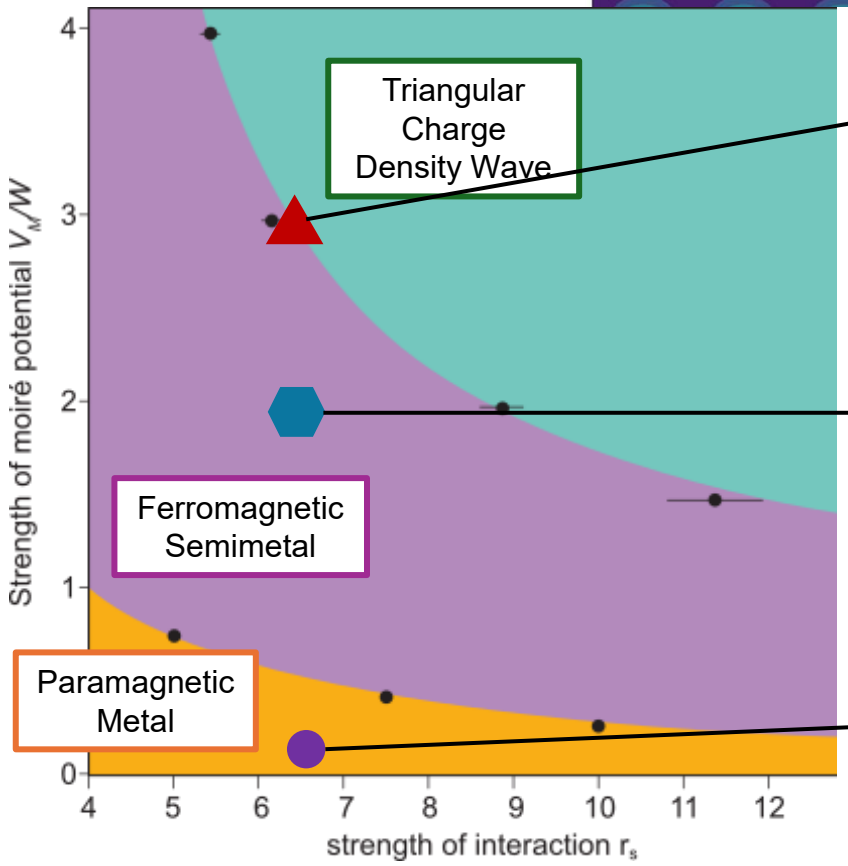

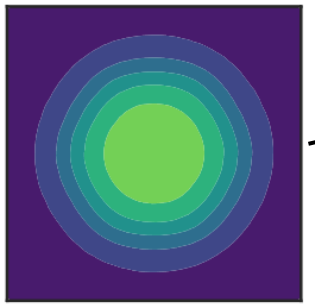

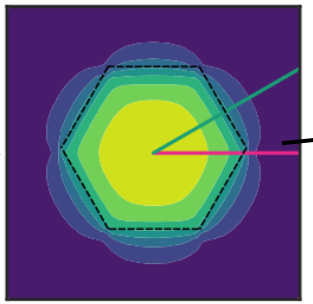

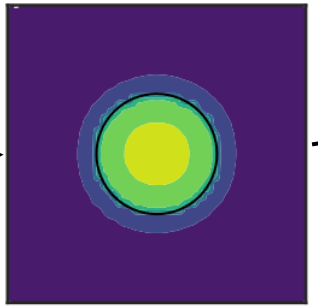

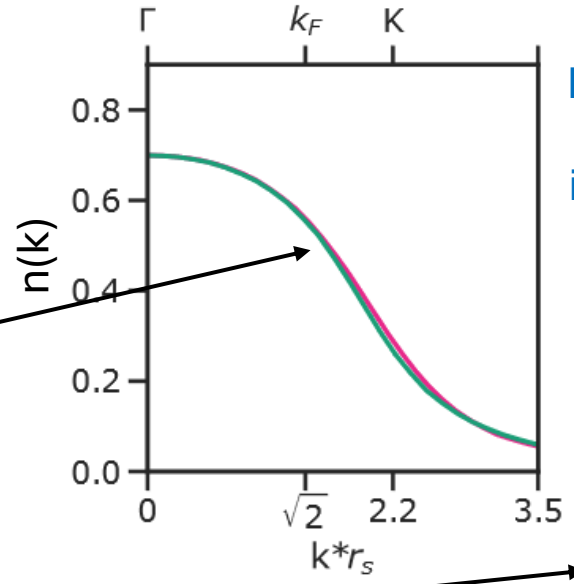

Insulator nearly isotropic

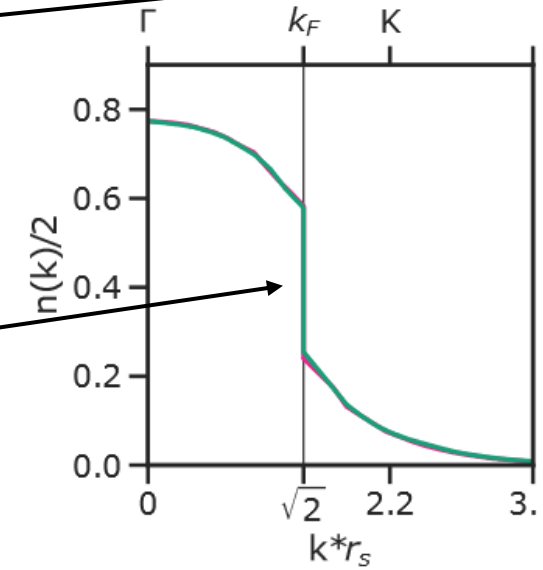

paramagnetic metal nearly isotropic

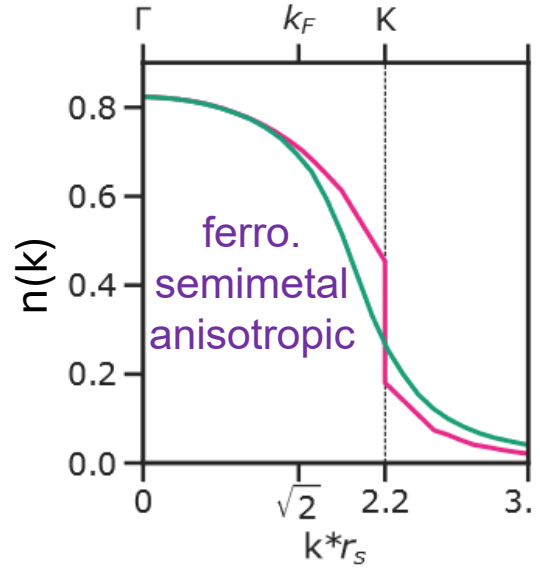

arXiv: 2406.01715

Y. Yang, M.A. Morales, S. Zhang, Phys. Rev. Lett. **133**, 266501 (2024)

Correlation functions from QMC provide deeper insight

Charge density retains honeycomb symmetry in all three phases

Pair correlation reveals broken symmetry in CDW phase

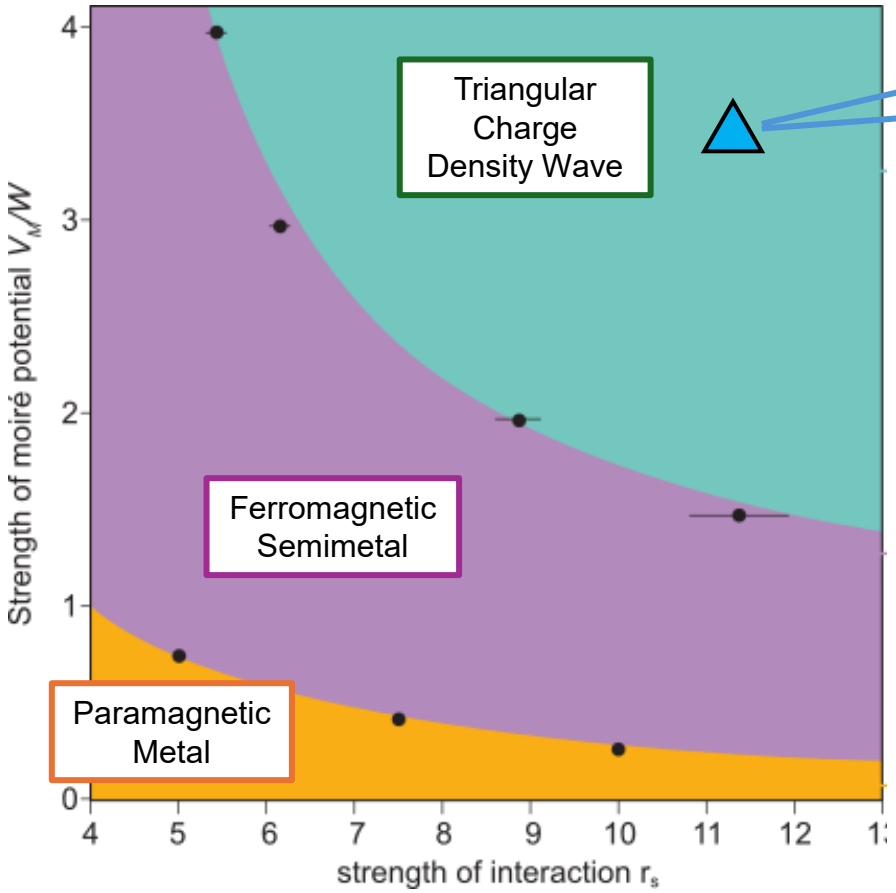

charge density

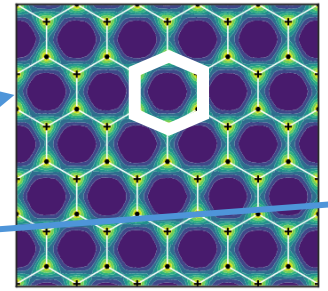

pair correlation

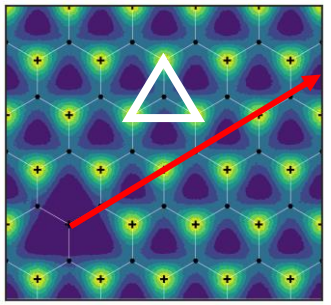

pair correlation linecut

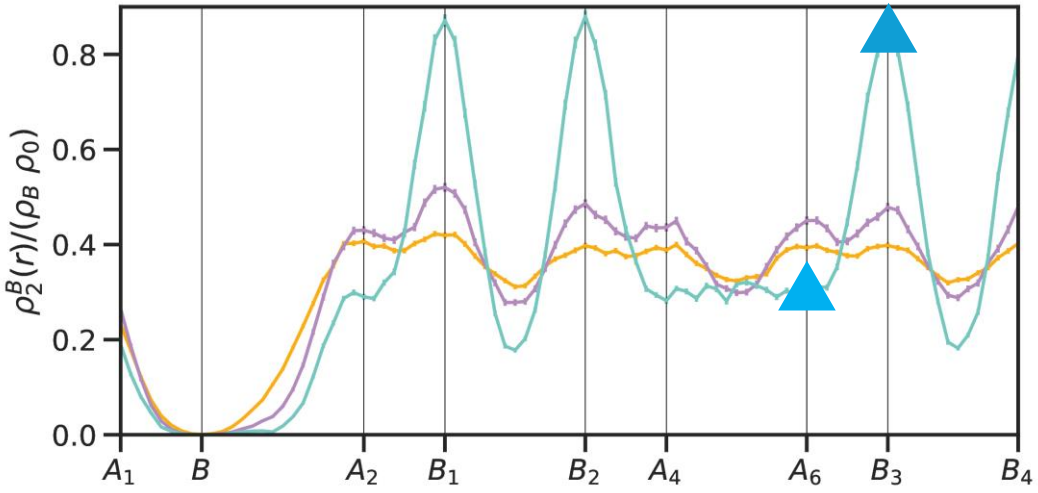

Y. Yang, M.A. Morales, S. Zhang, Phys. Rev. Lett. **133**, 266501 (2024)

Projector QMC, e.g. DMC, rely on qualitatively correct trial WF

LDA self-interaction error: one electron pushes itself apart favors metallic phase

Alleviate using non-local hybrid functional $E_{xc}^{hybrid} = \alpha E_x^{HF} + (1-\alpha)E_x^{LDA} + E_c^{LDA}$

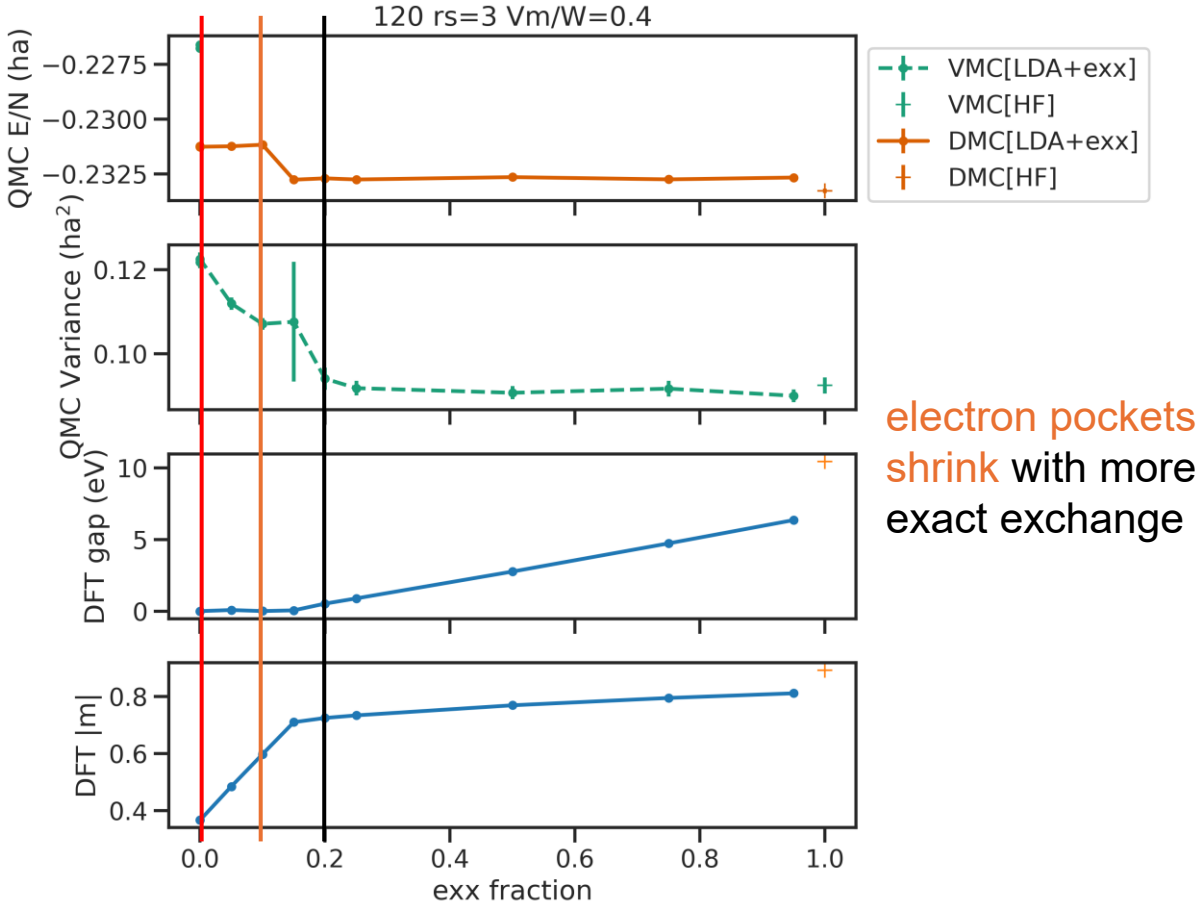

electron pockets shrink with more exact exchange

Momentum distribution shows electron pockets due to indirect band gap closure

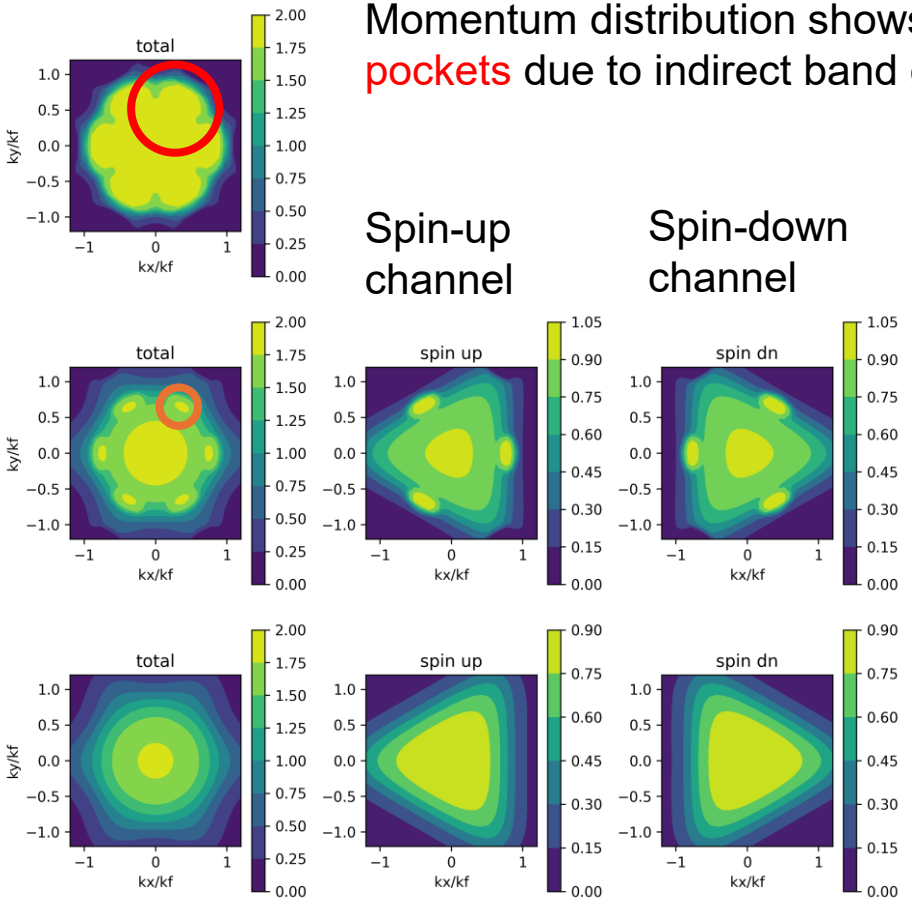

Looking into the Future: Incorporate Machine Learning/AI Tools

ChatGPT (o4-mini-high)

Draw a photo-realistic picture of a physicist looking into a crystal ball to predict the future of electronic structure theory and materials science.

See poster by Conor Smith

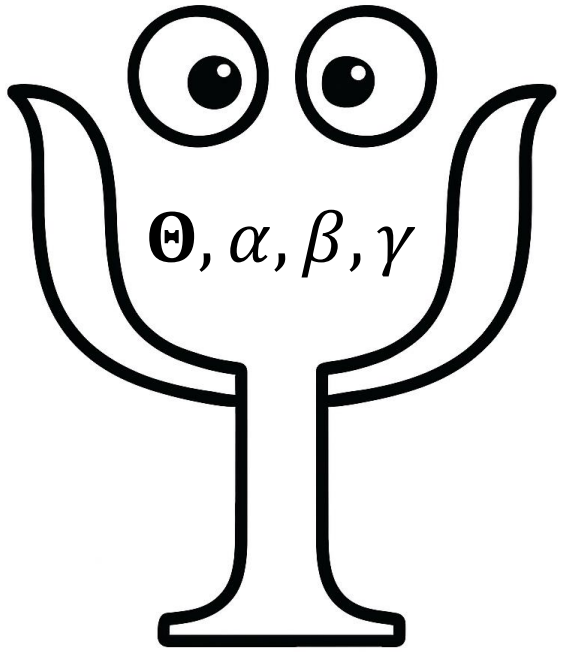

Conventional Trial wavefunction, a.k.a., variational ansatz

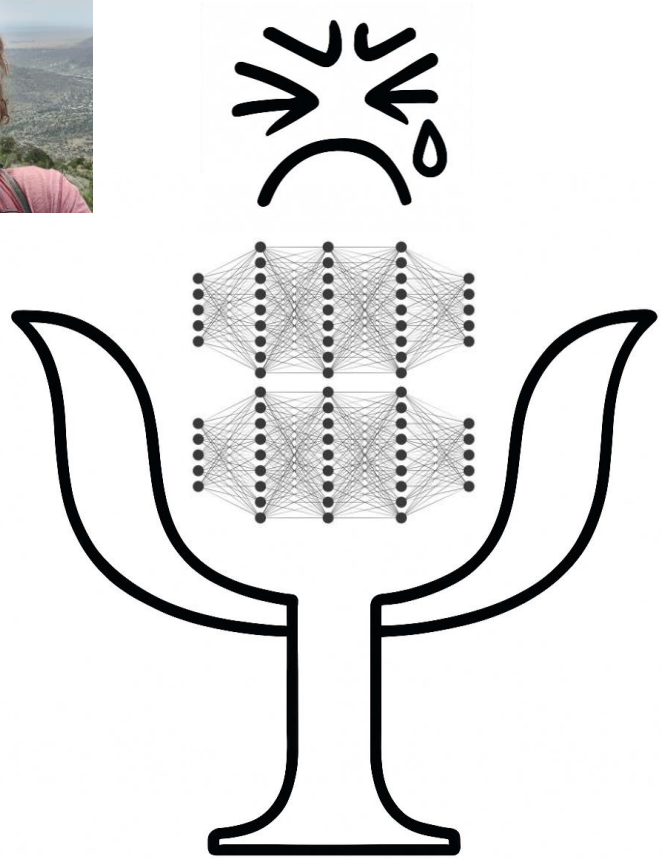

Neural Quantum State

The tree of transition metal dichalcogenide (TMD) moiré materials

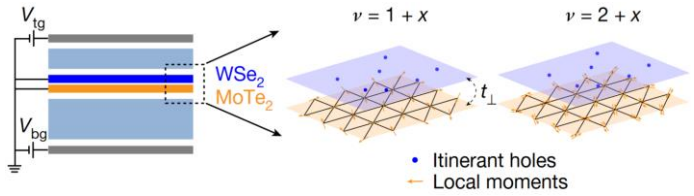

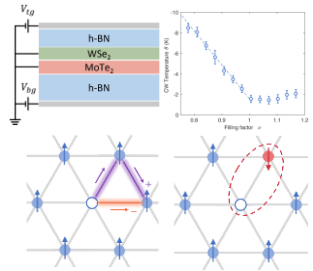

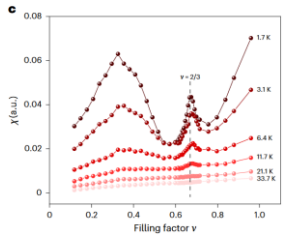

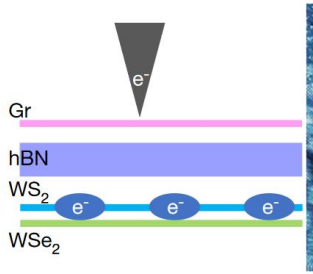

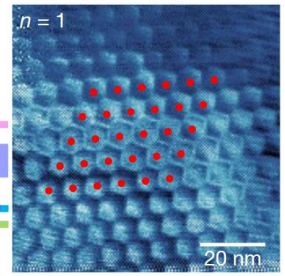

Kondo heavy fermion

interlayer coupling

external fields

topological superconductor

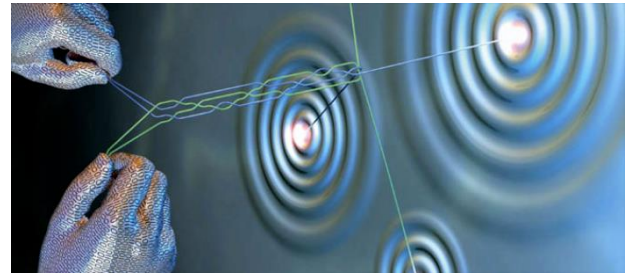

kinetic magnetism

temperature

Intralayer tunneling

fractional Chern insulator

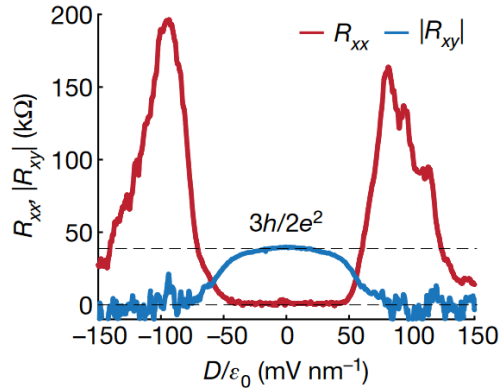

frusrated magnetism

screened interaction

filling

generalized Wigner crystal

Crystal of moiré "atoms"

moiré "helium"

moiré "lithium"

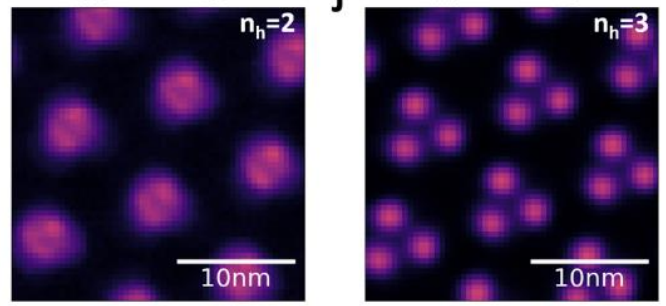

monolayer T=0 K

Summary of 2DEG in commensurate moiré potential

- Pin WC at higher density, where magnetic interaction is strong
- Triangular moiré favors AFM, while honeycomb moiré favors FM
- Correlation function offers deeper insight into the triangular CDW

- Recent analytical calculation (instanton) supports FM in honeycomb moiré thanks to unfettered 3-particle ring exchange

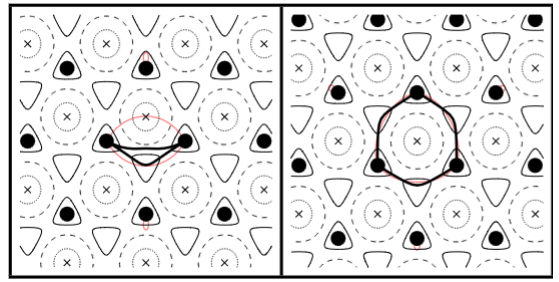

I. Esterlis and A. Levchenko
arXiv: 2502.00323

$WSe_2/MoSe_2$ → triangular moiré potential

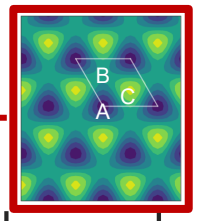

2306.14954

honeycomb moiré potential

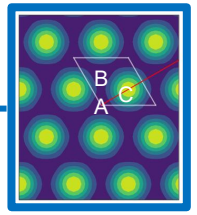

2406.01715